OXYGEN ISOTOPIC IMAGING OF A HIBONITE-GROSSITE-RICH INCLUSION FROM THE MILLER RANGE (MIL) 090019 CO3 CHONDRITE.

P. Mane[1,2] , A. N. Nguyen[2,3], J. J. Barnes[2], A. W. Needham[2,3], S. Messenger[2], D. K. Ross[2,3] and J. I. Simon[2], [1]Lunar and Planetary Institute, USRA, 3600 Bay Area Boulevard, Houston, TX 77058 USA (pmane@lpi.usra.edu), [2]Robert M Walker Laboratory for Space Science, EISD/Astromaterials Research Exploration Sciences, NASA Johnson Space Center, 2101, NASA Parkway, Houston, TX 77058 USA, [3]Jacobs, Houston, TX, 77058, USA.

Introduction: Calcium-Aluminum-rich Inclusions (CAIs) in primitive meteorites are the first solids to condense in the Solar System [e.g., 1, 2]. The oxygen isotopic compositions recorded in various mineral components of CAIs provide clues about their origin and post-formation history [e.g., 3], including processes such as condensation, melting, nebular alteration, and fluid-rock reactions on the parent body. Among primitive meteorites, CO3 carbonaceous chondrites are one of the minimally altered and the CAIs within them retain records of their earliest histories. Here we report results from oxygen isotopic imaging of a grossite-hibonite bearing CAI (CAI 44) from the Miller Range (MIL) 090019 CO3 chondrite, using NanoSIMS. The goal of this study is to search for evidence of nebular processes in phases that are most susceptible to parent body alteration.

Methods: The mineralogical and petrological characterization of CAI 44 was performed using the JOEL Hyperprobe 8530 electron microprobe at NASA JSC. Oxygen isotopic imaging of the CAI was done using the Cameca NanoSIMS 50L ion microprobe at NASA JSC. We followed the analytical protocol described in [4]. O-isotopic maps of the CAI were acquired by rastering a ~3 pA primary Cs^+ beam at 16 keV over an area of 20 × 20 µm over a period of ~7 hours. Negative secondary ions of $^{16}O^-$, $^{17}O^-$, $^{18}O^-$, $^{28}Si^-$, $^{24}Mg^{16}O^-$, $^{27}Al^{16}O^-$, and $^{40}Ca^{16}O^-$ were simultaneously acquired using electron multiplier detectors at a mass resolving power of >10,000, sufficient to resolve the $^{16}OH^-$ interference from the $^{17}O^-$ peak. An electron flood gun was used to mitigate sample charging during the analyses. We used San Carlos olivine and Madagascar hibonite as isotopic standards to correct for the instrumental mass fractionation. The O-isotopic ratios were corrected for the quasi simultaneous arrival (QSA) effect and the detector dead time.

Results and Discussion: CAI 44 contains a grossite and hibonite-rich core with spinel and perovskite grains. This core is surrounded by a melilite layer followed by a thin diopside layer. This CAI has some alteration products including sodalite and Fe-, Zn-rich spinel (hercynite). The O-isotopic compositions of the refractory phases grossite, hibonite, spinel, melilite, as well as the alteration phase Fe-, Zn-rich spinel, and the meteorite matrix are shown in Figure 1. The spinel and hibonite have ^{16}O-rich compositions as expected [5]. The melilite layer surrounding the CAI interior has an intermediate O-isotopic composition. The core grossite exhibits a ^{16}O-poor composition, plotting at the intersection of the terrestrial fractionation (TF) line and the carbonaceous chondrite anhydrous minerals (CCAM) line. The Fe-rich spinel grains derived from grossite [6] exhibit O-isotopic compositions close to the meteoritic matrix. This suggests that the formation of grossite and its alteration phases involved a more complex scenario than simply a fluid-rock interaction on the meteorite parent body. These observations suggest that the O-isotopic variation seen in the different CAI minerals likely recorded distinct nebular reservoirs as the CAI formed, consistent with the O isotope analysis of a spinel-rich CAI from the same meteorite [7].

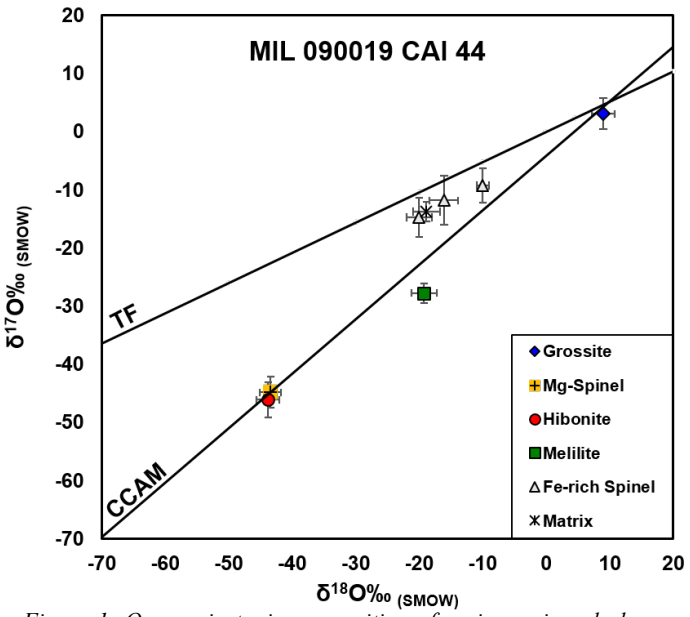

Figure 1: Oxygen isotopic composition of various mineral phases in CAI 44. Errors shown here are 1σ.

References: [1] Amelin Y. et al. (2010) *EPSL*, 300; 343-350, [2] Connelly J. N. et al. (2012) *Science*, 338: 651-655.[3] Yurimoto H. et al., (1998) Science 282 (5395), 1874-1877. [4] Ito M. & Messenger S. (2008) *Appl. Surf. Sci.* 255: 1446-1450. [5] Simon S. B. et al., (2019) *MAPS* https://doi.org/10.1111/maps.13282 [6] Maruyama S. & Tomioka N. (2011) *MAPS*, 46: 690-700. [7] Simon J. I. et al., (2017) *MAPS* 52: A325.